Biochemical Genetics (2019) 57:540–554
https://doi.org/10.1007/s10528-019-09907-3

ORIGINAL ARTICLE

A Novel CNGA1 Gene Mutation (c.G622A) of Autosomal Recessive Retinitis Pigmentosa Leads to the CNGA1 Protein Reduction on Membrane

Qing Gao[1] · Yifan Liu[1] · Xinlan Lei[1] · Qinqin Deng[1] · Yongqing Tong[2] · Lique Du[3] · Yin Shen[1]

Received: 26 June 2018 / Accepted: 9 January 2019 / Published online: 16 January 2019

Abstract

CNGA1 encodes a membrane protein on rod photoreceptor related to phototransduction. The present study was to identify a novel mutation of *CNGA1* associated with autosomal recessive retinitis pigmentosa by using next generation sequencing of a Chinese family. Next generation sequencing and Sanger sequencing has identified a compound heterozygous mutation in *CNGA1* gene, c0.472 del C (reported) and c0.829G>A (novel mutation, same as c0.622G>A according to NM_000087.3) of the proband. SIFT and Polyphen-2 predicted the *CNGA1* G622A site to be possibly deleterious. Evolutionary conservation analysis of amino acid residues showed this aspartic acid is highly conserved between species, and protein structure prediction by I-TASSER server indicated that the D208N mutation induced a large disappear of interactions between S2 and S4. Flag-tagged *CNGA1* and mutant G622A cDNA were generated and inserted into pCIG-eGFP vectors. Transfection of human embryonic kidney 293T cells was performed with lipofectamine. Interestingly, western blot and immunofluorescence results indicated that the expression of mutant CNGA1 (D208N) decreased significantly, especially on the membrane of transfected HEK293T cells. The novel variant c0.622G>A (p. D208N) in this study enriched the *CNGA1* mutation spectrum. Besides, this mutant was predicted "possibly damaging" due to bioinformatics analysis and validated by laboratorial experiments. Our study suggests that this mutation lead to the CNGA1 protein reduction from the cell membrane.

Keywords Retinitis pigmentosa · Cyclic nucleotide gated channel alpha 1 · Next generation sequencing

Electronic supplementary material The online version of this article (https://doi.org/10.1007/s10528-019-09907-3) contains supplementary material, which is available to authorized users.

✉ Yin Shen
yinshen@whu.edu.cn

Extended author information available on the last page of the article

Introduction

Retinitis pigmentosa (RP; OMIM 268,000) is a group of retina degenerative diseases with chronic, progressive degeneration of retinal pigmented epithelium and photoreceptors, with about 2.5 million people affected worldwide (Dias et al. 2018). It is highly genetic heterogeneous and exhibits various clinical phenotypes. Typical symptoms of RP include night blindness, peripheral visual fields loss, leading to tunnel vision and blindness. Clinical ophthalmic examinations show bone-spicule deposits, optic disk atrophy, attenuated retinal blood vessels, visual field loss, and diminished, or non-recordable electroretinography responses. So far, RP has been mapped to 87 identified genes (RetNet; https://sph.uth.edu/retnet/sum-dis.htm, last updated August 17, 2018), including autosomal dominant (ADRP), autosomal recessive (ARRP), and X-linked (XLRP). Hence, it is important to combine the genetic diagnose together with the clinical finding, to diagnose and treat RP precisely in the future.

Cyclic nucleotide gated (CNG) channel is involved in the visual phototransduction, whose family comprises six homologous members in mammals, A-type subunits (CNGA1–4) and B-type subunits (CNGB1 and CNGB3). A-type subunits can form functional homomeric channels in heterologous expression systems, while B-type subunits traffic the channel to the outer segment and co-assemble with A-type subunits to modulate their properties (James and Zagotta 2018; Kaupp and Seifert 2002). In rod photoreceptors, this channel has a 3:1 CNGA1:CNGB1 stoichiometry, while cone photoreceptors CNG channel consists of 3 CNGA3 and 1 CNGB3 (Weitz et al. 2002; Zhong et al. 2002). The CNG channel is located in the photoreceptor membrane. The CNG channel is maintained in the open state in the dark by binding high concentration of cGMP, allowing Na^+ and Ca^{2+} influxing, thus depolarizing the rod photoreceptors and promoting glutamate releasing into the synaptic gap. When the rhodopsin absorb a photon, the cGMP specific phosphodiesterase (PDE) is activated, hydrolyzing the cGMP, closing the CNG channel and hyperpolarizing the rod photoreceptor (Kramer and Molokanova 2001; Pepe 2001). *CNGA1* (OMIM 123,825) encodes a six transmembrane protein in the rod plasma membrane, defects in this gene will lead to retinitis pigmentosa autosomal recessive (ARRP) disease, RP49.

In this study, we identified a compound heterozygous *CNGA1* mutation c0.829G>A (same as 622G>A) and c0.472delC (NM_001142564.1) in a Chinese ARRP family. A combined approach of NGS and Sanger sequencing was used to identify the true mutation. Our finding reported a novel missense mutant position of *CNGA1* of ARRP which has never been reported before, enlarged the spectrum of *CNGA1* mutation and revealed a potential mechanism of RP.

Materials and Methods

Family Ascertainment

A 26-year-old girl with night blindness and narrow vision field visited us together with her non-symptomatic parents. Comprehensive ophthalmological examinations

including best correct visual acuity, fundus examination, vision field examination, macular optical coherence tomography (OCT), and electroretinogram (ERG) were performed with the proband. Genomic DNA was prepared from the proband and her parents peripheral blood and send to the BGI (Beijing Genomics Institute) for NGS and Sanger sequencing validation.

The research followed the tenets of the Declaration of Helsinki, and was approved by the Ethics Committee of Renmin Hospital of Wuhan University. Informed consent was obtained from the family.

Next Generation Sequencing and Sanger Sequencing Validation

A custom-made capture array designed by the BGI, was used to capture the exons coding 67 RP-related genes. Genomic DNA from proband was fragmented ranging from 200 to 250 bp. The primers, adapters, and indexes were then ligated to the DNA fragments to construct libraries. The DNA fragments were pooled and hybridized to the custom capture array. After hybridization, the captured library was sequenced on the HiSeq2000 Analyzer (Illumina) to generate paired-end reads. Next, the raw reads (sequencing data generated from the HiSeq2000) were filtered as clean reads and then aligned to the GRCh37 (hg19) human reference sequence with the Burrows–Wheeler aligner (Li and Durbin 2010). Single-nucleotide polymorphisms (SNPs) and indels frequency were annotated by databases such as dbSNP (https://www.ncbi.nlm.nih.gov/projects/SNP/), the 1000 Genomes (https://www.internationalgenome.org/) and a database of 128 normal residents from BGI. Remaining mutations were analyzed using the protein harmfulness prediction programs Polyphen-2 (Adzhubei et al. 2010) and sorting intolerant from tolerant (SIFT) (Kumar et al. 2009). For Sanger sequencing, primers for *CNGA1* were designed to amplify and sequence the mutant exons of the gene according to RefSeq transcript NM_001142564.1 (see Supplementary Table for primer sequences).

Conservation Analysis

To assess the conservatism of the CNGA1 protein, amino acid sequences from 15 different species were aligned by clustalW (Larkin et al. 2007) including human (NP_000078.2), Norway rat (NP_445949.1), house mouse (NP_031749.2), cattle (NP_776703.1), dog (NP_001003222.1), zebrafish (XP_701036.4), chicken (NP_990551.1), tropical clawed frog (XP_017950934.1), Rhesus monkey (XP_014993822.1), northern white-cheeked gibbon (XP_003258470.1), Sumatran orangutan (XP_009238212.1), horse (XP_005608848.1), rabbit (XP_008246828.1), chimpanzee (XP_016800416.1), and goat (XP_017905432.1).

Molecular Modeling

We uploaded the wild-type and mutant (D208N) CNGA1 protein sequences to the I-TASSER server (https://zhanglab.ccmb.med.umich.edu/I-TASSER/) to predict the possible protein structures. Then we used the SWISS-PDB software (https://spdbv

.vital-it.ch/disclaim.html#) to visualize these protein structures. The models were viewed in ribbon and backbone styles to display the helixes and residues clearly.

Protein Expression

Flag-tagged (DYKDDDDK) CNGA1 (NM_000087.3) were inserted between XhoI and EcoRI restriction-endonuclease sites in pCIG vector, and an eGFP reporter was carried behind the IRES2 sequence in this vector. The G622A mutant was generated by PCR. The plasmids were confirmed that the mutagenesis occurred correctly by sequencing. Human embryonic kidney (HEK) 293T cells (ATCC) were chosen for transfection due to its transfectability and low self-expression of CNGA1. Cells were maintained in DMEM (Gibco, Life Technologies) supplemented with 10% FBS (Multicell, Wisent Inc) in 5% CO_2 at 37 °C. Cells were transfected with Lipofectamine™ 2000 transfection reagent (Invitrogen) at around 80% confluence, incubated for 6–8 h, washed out, then cultured with DMEM and 10% FBS for an additional 32 h before harvest.

Immunocytochemistry

Cells were cultured at 0.1% gelatin pre-treated slides in 24-well plates. 0.5 µg plasmid and 1.5 µl Lipofectamine were diluted with 100 µl Opti-MEM respectively for 5 min, then mixed together for 15 min at room temperature. Transfection procedures were described as above. After transfection, they were fixed in 4% paraformaldehyde for 10 min and blocked with 0.2% BSAT (5 g bovine serum albumin and 0.2 ml Triton dissolved in 100 ml PBS) for 40 min at room temperature free of light; then incubated with primary antibodies against FLAG (1:100; MBL, PM020) overnight at 4 °C. After 3 times wash in 0.01 mol/l PBS, the cells were subsequently incubated with Cy3-conjugated secondary antibodies (1:200; Antgene, ANT030) for 1 h at RT. After another 3 times wash with PBS, the cells were incubated with DAPI (1:100) for 5–10 min. Images were taken using the laser scanning confocal microscope (Olympus FV1200).

Western Blot

For each well of 6-well plates, 6 µg plasmid and 5 µl Lipofectamine were diluted into 1.6 ml Opti-MEM. The total protein of wild-type and mutant groups were extracted from transfected HEK293T cells using RIPA (Servicebio, G2002) and PMSF (Servicebio, G2008) compound lysis buffer (100:1) on the ice. The membrane protein was extracted according to the ProteinExt Mammalian Membrane Protein Extraction Kit (transgen) instruction. The protein content in the sample was measured by the BCA assay and adjusted to about 30 µg per well. These proteins were separated by 10% SDS-PAGE electrophoresis and transferred to nitrocellulose membrane. The membrane was kept in blocking buffer (5% non-fat milk in TBST) for 1 h at room temperature, then incubated overnight at 4 °C with rabbit anti-DDDK-tag antibody (1:1000; MBL, PM020), rabbit anti-GAPDH antibody (1:6000; Antgene, ANT012),

rabbit anti-NaK ATPase antibody (1:10,000; abcam, Ab76020), and rabbit anti-β-tubulin antibody (1:1000; Sigma, SAB4500088). After three 10-min washes with 0.01 mol/l TBST, the nitrocellulose membrane was probed with goat anti-rabbit secondary antibody conjugated with horseradish peroxidase (HRP; 1:8000; Servicebio, GB23303) at room temperature for 90 min. Then the membrane was washed 5 min for 3 times with TBST. Immunoreactive bands were subsequently detected using ECL reagents and recorded by X-ray films.

Statistical Methods

ImageJ Fiji (Schindelin et al. 2012) and Adobe Photoshop CC were used for cell counting and western blot analysis respectively. Mann Whitney test were used to determine significant differences between wild-type and mutant groups. All western blot bands were normalized using GAPDH. Data were analyzed and graphed using Graphpad Prism software version 7 (Graph Pad Software Inc., La Jolla, CA, USA), and represented as means ± SD. $p < 0.05$ was statistically significant.

Results

Patient Phenotype

The proband underwent night blindness at childhood with peripheral vision field loss at the age of 26. Her best correct visual acuity is 20/20 at both eyes. The fundus image showed a pale peripheral area with no obvious deposits at the posterior pole (Fig. 1a). Humphrey Visual Field Analyzer demonstrated central vision field residual of both eyes (Fig. 1a). Macular OCT is normal (Fig. 1c). The ERG presented extinguished responses with significant decline of a and b amplitudes (Fig. 1d). Her family history has no night blindness, vision field loss, or any other RP associated symptoms.

Identification of CNGA1 Mutation

The custom-made capture array involved 67 inherited retinal disease related genes. The mean depth and coverage for CDS1–9 of *CNGA1* was shown in Fig. 2a. The total average depth was 278.5-fold and the coverage was 99.52%. After the removal of common variants from the databases in methods, non-pathogenic variants based on SIFT/PolyPhen-2 from 107 SNPs and indels, the candidate SNPs/insertions/deletions of known RP gene were concluded to *CNGA1*: chr4: 47,942,822 substitutions in exon9 and chr4: 47,951,883 indel in exon5 (according to the hg19). The *CNGA1* exon5 chr4: 47,951,883 indel could be transcribed to c0.472delC (NM_001142564.1) and translated to cause a frameshift p.(L158Ffs*4): 158 position leucine was replaced by the phenylalanine with a result of a premature termination. This small homozygous deletion c0.472delC has been reported in 2015 (Yang et al. 2015). The *CNGA1* exon9 chr4 47,942,822 missense variant was predicted

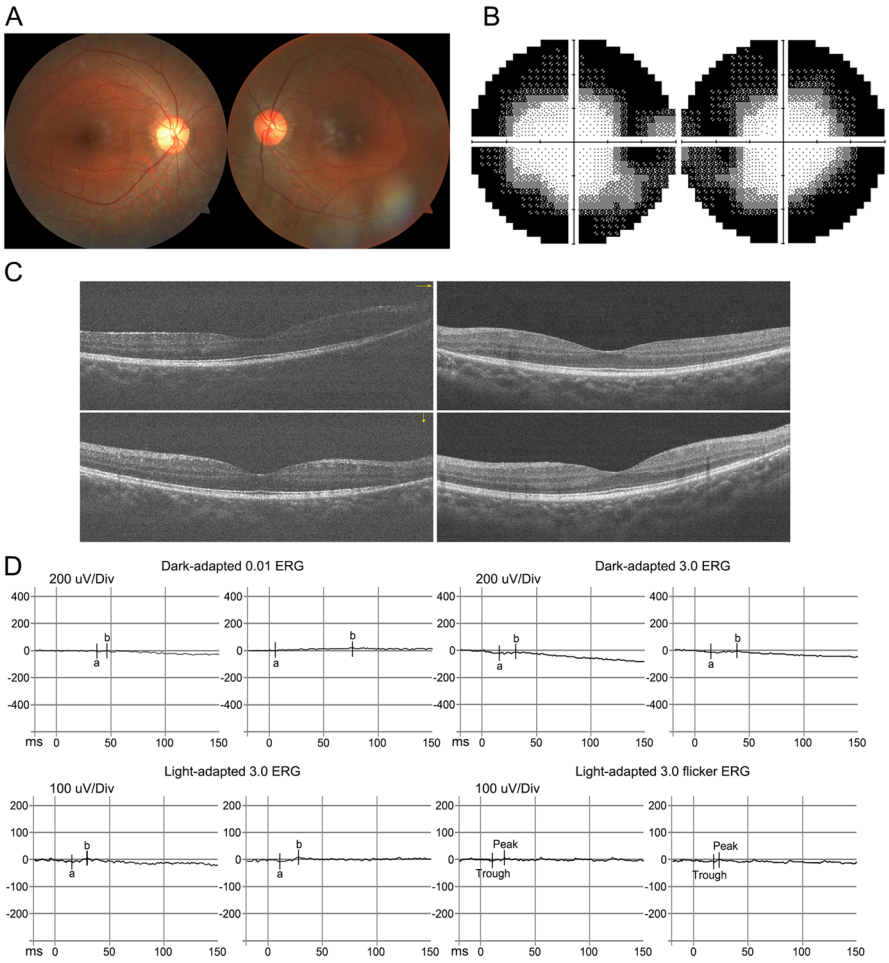

Fig. 1 Ophthalmological exam of the proband. **a** The fundus image demonstrates a pale peripheral area with no obvious deposits at the posterior pole. **b** The proband showed a tunnel vision field of both eyes, reminiscent of the pale surrounding of macular in fundus images. **c** The macular OCT showed a quite regular macular structure of the proband. **d** The full-field ERG examination revealed nearly extinguished responses, indicating the degeneration of the photoreceptors

to cause c0.829G>A (p.D277N) according to NM_001142564.1 or c0.622G>A (p.D208N) according to NM_000087.3, as a result, the aspartic acid was replaced by asparagine. Functional effect prediction of the mutation was carried out by the online tool SIFT, PolyPhen-2 and PROVEAN (Choi and Chan 2015), indicating "damaging", "possibly damaging" and "deleterious" with scores of 0.011, 1.000 and −4.83 respectively. These two SNPs frequencies were 0 in whole samples of database of 1000 Genomes Project and haven't been reported up to now.

To validate the *CNGA1* mutations and the inheritance pattern of RP in the family, Sanger sequencing was used to analyze the variants in the proband and her parents.

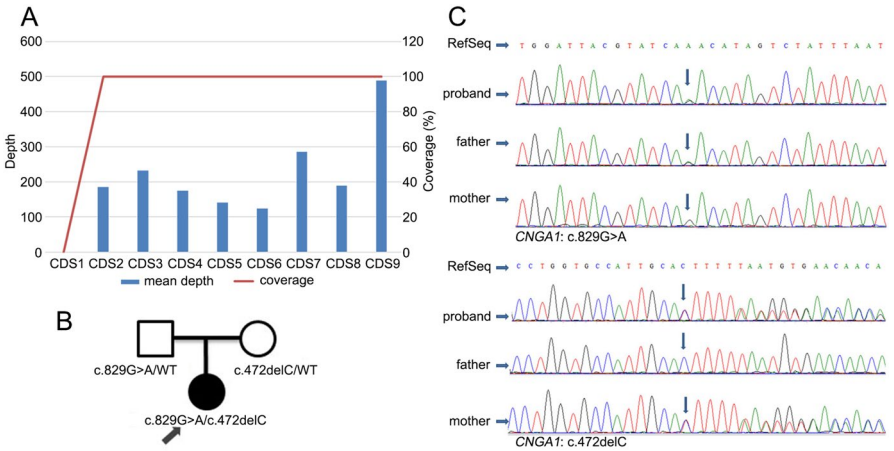

Fig. 2 Identification and confirmation of the compound heterozygous mutation c. G829A (same as 622G>A) and c0.472delC in *CNGA1* in a Chinese family with ARRP. **a** The average sequencing depth and coverage for CDS1–9 in the *CNGA1* gene. **b** Family pedigree. The patient pointed by the arrow is the proband. **c** The heterozygous *CNGA1* mutations identified by Sanger sequencing. The arrows indicate the site of mutations

The sequencing results demonstrated that the proband and her father had detected heterozygous c0.829G>A (same as 622G>A) mutation, whereas the proband and her mother detected heterozygous c0.472delC (Fig. 2c). The proband's parents both carried a *CNGA1* mutation which led to a compound heterozygous mutation in the proband, corresponding to the autosomal recessive inheritance pattern of RP49 associated with *CNGA1* (Fig. 2b).

Evolutionary Conservation Analysis

We compared the human and other species (see "Methods") of the CNGA1 protein. Homologous peptides sequences from 15 species were aligned to identify the conservation of the mutate residue (Fig. 3a). The alignment implied that the aspartic acid at position 208 is highly conserved between species, and the change of the position may play an important role in the function of CNGA1.

In Silico 3D-Structure Prediction

Possible structures of the wild-type and mutant human CNGA1 protein were predicted by I-TASSER server using PDB 5H3O chain A (*C. elegans* CNGA TAX-4) as the template and visualized by SWISS-PDB software. The mutant position 208 located in an α-helix structure of the second transmembrane domain (S2) from the N terminal. The c0.622G>A nucleotide substitution led to a replacement of aspartic acid (D) by asparagine (N) at the 208 residue of the CNGA1 protein. In the TAX-4 channel, there are extensive interactions formed between conserved aspartic acid

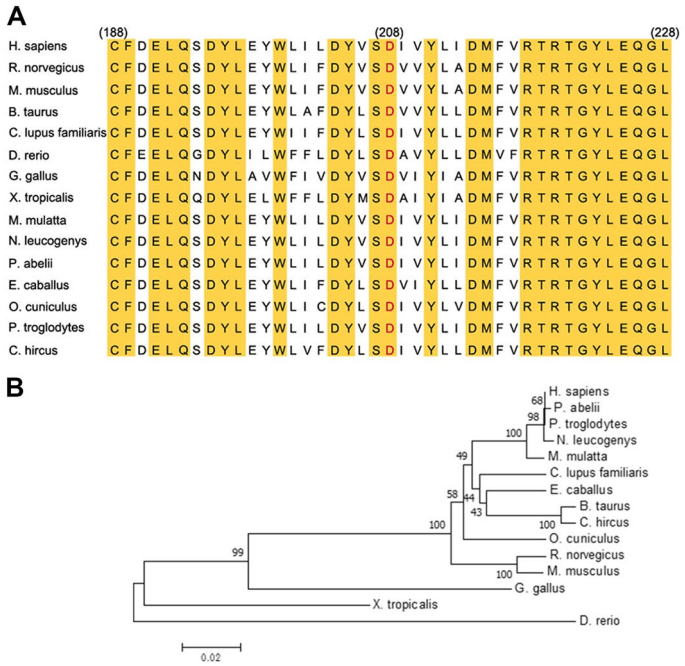

Fig. 3 The evolutionary conservation analysis of CNGA1 protein in multiple species. The c. G622A (p. D208N) mutation identified in this patient is situated at a highly conserved position in CNGA1. **a** Alignment of CNGA1 proteins from different phyla. Selected CNGA1 proteins were listed in methods. Sequences were aligned by ClustalW program. Yellow background: the conserved residues; red letters/yellow background: the 208 residues of CNGA1. **b** Evolutionary relationships of taxa. The evolutionary history was inferred using the Neighbor-Joining method. The percentage of replicate trees in which the associated taxa clustered together in the bootstrap test (1000 replicates) are shown next to the branches (Color figure online)

residues in S2 and conserved arginine residues in S4. These interactions may "serve to restrict the movement of S4b and stabilize S2″ (Li et al. 2017). In the wild-type model, these interactions are conserved: the negative D208 interacts with positive R271 (via a salt bridge) and R274 (Fig. 4a). However, in the mutant model, these interactions are largely changed: the salt bridge between the N208 and R271 disappeared, no interaction existed between N208 and R217, and H-bonds between S2 and S4 reduced significantly (Fig. 4b).

Laboratory Experiments

To evaluate the influence of this mutation in vitro, we generated wild-type and mutant *CNGA1* plasmids and transfected them separately in HEK293T cells. The *CNGA1* gene was tagged with FLAG before the polyA so that we could detect CNGA1 protein by anti-flag antibodies. For immunofluorescence staining, both wild-type and mutant CNGA1 protein could be efficiently expressed in HEK293T (Fig. 5a). Due to the transmembrane property of the CNGA1 protein, the wild-type

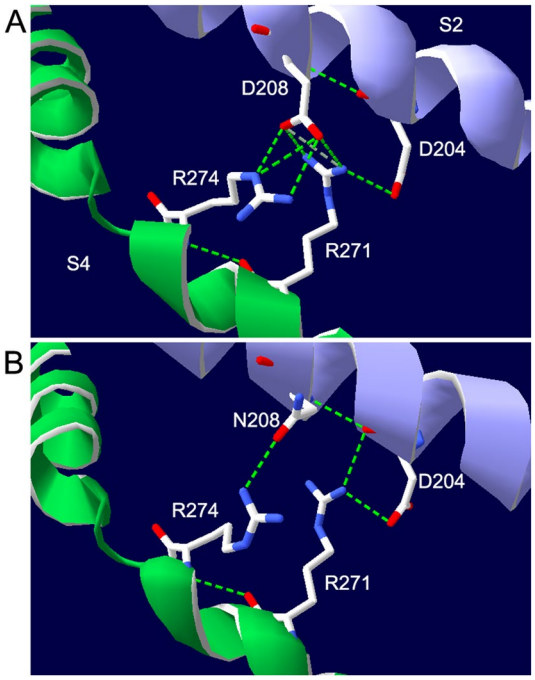

Fig. 4 CNGA1 protein molecular alteration caused by the *CNGA1* variant c0.622G>A (p. D208N). These models were predicted by I-TASSER server, using the 5h3o chain A (*C. elegans* CNGA TAX-4) as the template. The transmembrane domain 2 and 4 are shown in blue and green ribbons respectively while the positions D204, R271, R274 and mutant residue 208 are displayed as backbones. **a** In the wild-type model, the negative aspartic acids D208, along with D204 in the S2, are engaged in interactions with positive charges in S4, including R271 (via a salt bridge) and R274. **b** In the mutant model, the D208 residue was replaced by a neutral uncharged asparagine, with salt bridge disappeared and H-bonds (green dash line) between these residues decreased obviously. The C, O, N atoms are in white, red, and green color respectively (Color figure online)

CNGA1 protein is often localized to one or multiple cellular protrusions present in HEK293T cells (Fig. 5A1). Interestingly, the mutant CNGA1 protein fails to be localized to the cellular protrusions (Fig. 5A2). However, it appears that expressing either the wild-type or mutant CNGA1 protein does not affect the formation of cellular protrusions in HEK293T cells (Fig. 5d). These transfected cells are divided into five categories by the numbers of protrusions (CNGA1 expression) under fluorescence image: 0, 1, 2, 3, >3 cellular protrusions (Fig. 5b), and summarized in Fig. 5c. A majority (81.3%) of wild-type HEK293T cells express CNGA1 protein in protrusions, while 66.5% G622A mutant group cells have no protrusions expression (Fig. 5c).

To further decide whether the CNGA1 protein decreased on the membrane, we collected the total protein and extracted the membrane protein of transfected cells, immunoblotted them with Flag (for CNGA1) antibodies. The CNGA1 protein could be detected around 79 kDa. The expression of NaK ATPase, GNGA1, GAPDH, and

Fig. 5 Expression of D208N mutant CNGA1 protein decreased on the cellular protrusions. CNGA1 tagged with Flag, fluorescence image represents the expression of CNGA1 protein. **a** Wild-type and D208N mutant CNGA1 plasmids were expressed in the HEK293T cells. A1 and A2 were enlarged 2.5-fold from the white boxes of the left images respectively. **b** Representative cells with 0, 1, 2, 3 and> 3 protrusions (white arrows). **c** In the wild-type group, CNGA1 express abundantly in HEK cells, with 81.3% cells have protrusions, and with 36.4% express more than 3 protrusions. In D208N mutant CNGA1 group, Flag-tagged protrusions were dramatically decreased with 66.5% has no protrusion. The protrusions tagged with Flag represent the expression of CNGA1 protein. ($n = 17$, the p value of 0, 1, 2, and ≥ 3 protrusions groups were $p < 0.0001$, $p = 0.2486 > 0.05$, $p < 0.0001$, $p < 0.0001$ respectively, Mann Whitney test). **d** Overlay of CNGA1 fluorescence and bright field image. The wild-type cells displayed flag-tagged protrusions under fluorescence image corresponding to bright field. However, in the mutant group, cells maintained protrusions, didn't exhibit its protrusions with flag antibodies at fluorescence image, indicating that the CNGA1 protein decreased on the protrusions. The asterisks indicate the representative mutant cells, the triangles point to the cellular protrusions that doesn't express CNGA1 protein

absence of β-tubulin verified the purity of the extracted membrane protein. Consist with the immunofluorescence results above, the mutant CNGA1 protein significantly decreased both in total and membrane protein (Fig. 6).

Discussion

In the present study, a 28-year-old female Chinese patient experiencing early-onset night blindness, came to our hospital and complained with night blindness and peripheral vision field loss. The patient presented with night blindness, tunnel vision field and extinguished ERG waves, but her BCVA, OCT and fundus image appears to be normal, indicating a relatively mild phenotype among RP. From the follow-up study, the vision field loss of the proband didn't further aggravate one year after the incipience. Using a strategy entailing a custom-made array and Sanger sequencing of the candidate chromosomal region we identified a novel mutation in RP-related gene: *CNGA1* on chromosome 4: 47,942,822, c. G622A, p(D208N). *CNGA1* is one of autosomal recessive RP-related genes that encodes a cGMP-binding transmembrane channel in rod photoreceptor. Next, we employed bioinformatics methods and predicted the p.(D208N) mutation to be pathogenic and evolutionarily highly conserved among diverse species, illustrating that it is important for protein function. We further explored the structure transformation of the mutant protein in silico, 3D structural modeling revealed an obvious interaction alteration between S2 and S4. These disappeared interactions, especially the salt bridge, might influence the stabilization of S2 and S4. Moreover, we constructed and transfected wild-type and mutant (G622A) *CNGA1* plasmids into HEK293T cells to investigate the potential pathogenic mechanism of this variant. The plasmids containing the p.(D208N) mutation encoded the full-length protein, however, the CNGA1 protein decreased significantly in the mutant group, the amount of expression on the cellular protrusions reduced either. By counting the protrusions under the fluorescence image of the wild-type and mutant 293T cells, we found that the mutant group exhibited fewer protrusions than the wild-type group. And the western blot results verified that the CNGA1 protein decreased on the membrane. Whether the reduced expression on the membrane is derived from mRNA instability or protein degradation need to

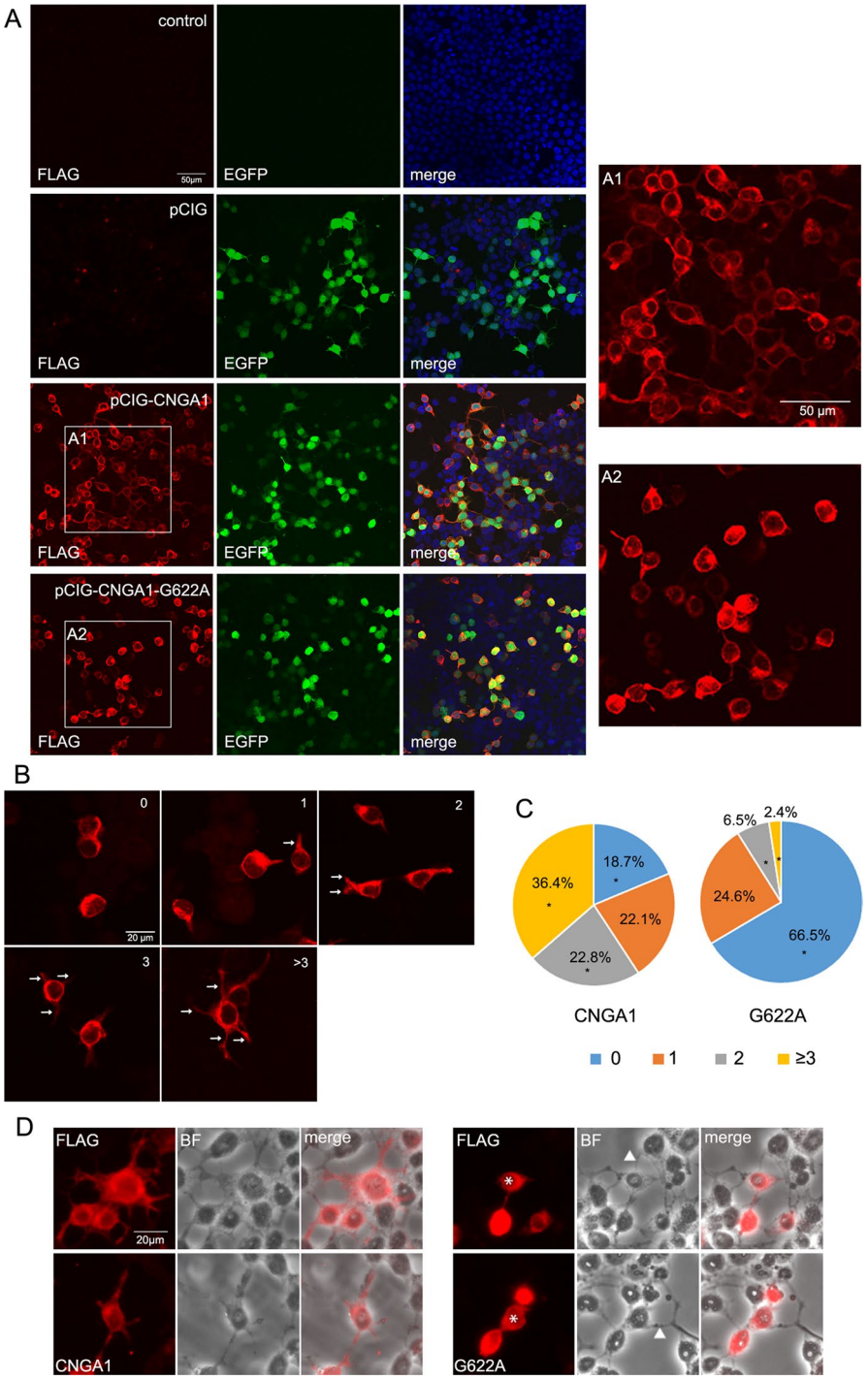
A
control
FLAG
50μm
EGFP
merge
pCIG
FLAG
EGFP
merge
pCIG-CNGA1
A1
FLAG
EGFP
merge
pCIG-CNGA1-G622A
A2
FLAG
EGFP
merge
A1
50 μm
A2
B
0
1
2
20 μm
3
>3
C
18.7%
22.1%
22.8%
36.4%
CNGA1
6.5%
2.4%
24.6%
66.5%
G622A
0
1
2
≥3
D
FLAG
BF
merge
20μm
CNGA1
FLAG
BF
merge
G622A

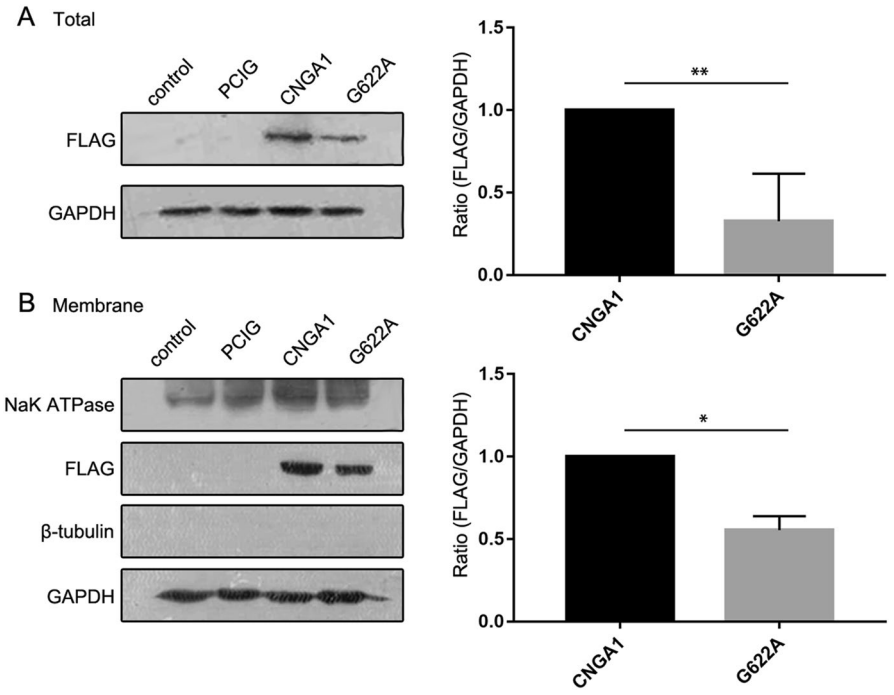

Fig. 6 The total and membrane CNGA1 protein decreased significantly. **a** Transfected cell total lysates demonstrated a significant CNGA1 protein reduction in mutant group. The right bar chart summarized the CNGA1 protein expression quantity of wild-type and mutant groups, $n=6$, $p=0.0022<0.05$, Mann Whitney test, mean ± SD. **b** The membrane protein expressed NaK ATPase, GNGA1, GAPDH without β-tubulin. The CNGA1 protein also decreased in the extracted membrane protein, $n=4$, $p=0.0286<0.05$, Mann Whitney test, mean ± SD

be further studied. In consequence, the c.G622A mutation led to CNGA1 protein reduction, especially on the membrane, which resulted in the lack of normal cGMP-gated cation channel in the rod photoreceptor membrane and subsequently affected the phototransduction.

CNG channels are a group of ion channels which are voltage dependent but are activated and opened by the intracellular binding of cyclic nucleotides (Kaupp and Seifert 2002; Matulef and Zagotta 2003), functioning in sensory transduction in the retina and olfactory epithelium (Biel and Michalakis 2009). Native rod photoreceptor CNG channel is a hetero-tetrameric protein composed of 3 CNGA1 subunits and 1 CNGB1subunit (Meighan et al. 2013; Pifferi et al. 2006). Thus, mutations in *CNGA1* may lead to phototransduction disorder and retinitis pigmentosa. By now, 14 mutations have been identified, including 10 missense/nonsense and 4 small deletions, all of them were associated with RP (https://www.hgmd.cf.ac.uk/ac/gene.php?gene=CNGA1).

Previous studies identified that a frameshift mutation in codon 645 of *CNGA1*, truncating the last 32 amino acids in the C terminus (Dryja et al. 1995), as with

another substitution c0.1537G>A (p.G513R) (Jin et al. 2016), were found to encode a protein that is predominantly retained inside the cell instead of being targeted to the membrane. In the present study, our immunofluorescence and western blot results showed a similar finding that the CNGA1 protein on the 293T cell membrane decreased. However, the mechanism how this mutation influences the protein level remains unclear. In animal model, mice overexpressing a *CNGA1* antisense mRNA with an about 50% reduction of *CNGA1* transcript levels are the first model of retinal degeneration caused by an alteration in the expression of CNG channel, and result in some histological features of photoreceptor and bipolar cells degeneration reminiscent of RP (Leconte and Barnstable 2000). Our results are in accordance with these finding that the down-regulation of CNGA1 affects rod-mediated vision. Future investigations using the electrophysiology accompany with immunohistochemistry methods may help address the molecular mechanism directly.

Several mutant positions have been described to influence the CNGA1 protein structure or function in previous studies. CNGA1 channel is a 690 amino acid protein, with six transmembrane α-helices (S1–S6) that span the lipid bilayer (Maity et al. 2015; Nair et al. 2009). The pore region is between S5 and S6, containing a selectivity filter (P367–T359), P-helix (V348–L358), and a loop between P-helix and S5 (F325–Y347). Previous study has shown that the S4 domain is mechanically coupled to S5 in the open state, but S3 in the closed state by means of single-molecule force spectroscopy (Maity et al. 2015). Residues constituted the selectivity filter such as T359, T360 and E363 were regarded as key binding sites controlling monovalent cations selectivity and permeation (Marchesi et al. 2012; Mazzolini et al. 2009). F380C (S6 domain) mutation is identified to form a disulfide bond between the exogenous C380 and the endogenous C314 (S5 domain) (Nair et al. 2006). Another mutation, P293A (S4–S5 linker), could affect ionic permeation and regulate the CNGA1 channel activation (Maity et al. 2015). Recent study has revealed that the opening of CNGA1 channels is initiated by the formation of salt bridges between residues in the C-linker and S5 helix (Mazzolini et al. 2018). Residues at different position play various roles, and an amino acid substitution may influence the entire protein function by affecting the transmembrane structure, unfolding of the loops between the transmembrane domains, ion permeation, cGMP binding, and so on. Mutations near C terminal got more studied and proved to be critical, while rare residues near N terminal were researched. But in our study, we detected a novel mutation D208N which is in S2 transmembrane domain near the N terminal. With this mutation, the interactions between S2 and S4 are largely disappeared. The loss of these interactions might lead to reduced stability of the transmembrane domain, and reduced membrane translocation. Also, the PH decrease inactivates the CNGA1 channel (Marchesi et al. 2015).

In conclusion, our study revealed a novel mutation of *CNGA1* in an ARRP family that has never been reported before, proved that this mutation led to CNGA1 protein reduction on the cell membrane, and provided a potential mechanism for RP that should direct future therapeutic approaches.

Acknowledgements We thank Ting Xie, the professor of the Stowers Institute for Medical Research for proof reading. We thank professor Xing Jian for the technique support in molecular modeling. Work was

funded by The National Nature Science Foundation of China (Grant No. 81470628), International Science and Technology Cooperation Program of China (2017YFE0103400) and Guangdong Provincial Key Laboratory of Ophthalmology and Visual Science (2017B030314025).

Compliance with Ethical Standards

Conflict of interest: The authors declare that they have no conflict of interest.

References

Adzhubei IA et al (2010) A method and server for predicting damaging missense mutations. Nat Methods 7:248–249. https://doi.org/10.1038/nmeth0410-248

Biel M, Michalakis S (2009) Cyclic nucleotide-gated channels. Handb Exp Pharmacol. https://doi.org/10.1007/978-3-540-68964-5_7

Choi Y, Chan AP (2015) PROVEAN web server: a tool to predict the functional effect of amino acid substitutions and indels. Bioinformatics 31:2745–2747. https://doi.org/10.1093/bioinformatics/btv195

Dias MF, Joo K, Kemp JA, Fialho SL, da Silva Cunha A, Jr., Woo SJ, Kwon YJ (2018) Molecular genetics and emerging therapies for retinitis pigmentosa: basic research and clinical perspectives. Prog Retin Eye Res 63:107–131.https://doi.org/10.1016/j.preteyeres.2017.10.004

Dryja TP, Finn JT, Peng YW, McGee TL, Berson EL, Yau KW (1995) Mutations in the gene encoding the alpha subunit of the rod cGMP-gated channel in autosomal recessive retinitis pigmentosa. Proc Natl Acad Sci USA 92:10177–10181

James ZM, Zagotta WN (2018) Structural insights into the mechanisms of CNBD channel function. J Gen Physiol 150:225–244. https://doi.org/10.1085/jgp.201711898

Jin X, Qu LH, Hou BK, Xu HW, Meng XH, Pang CP, Yin ZQ (2016) Novel compound heterozygous mutation in the CNGA1 gene underlie autosomal recessive retinitis pigmentosa in a Chinese family. Biosci Rep 36:e00289. https://doi.org/10.1042/BSR20150131

Kaupp UB, Seifert R (2002) Cyclic nucleotide-gated ion channels. Physiol Rev 82:769–824. https://doi.org/10.1152/physrev.00008.2002

Kramer RH, Molokanova E (2001) Modulation of cyclic-nucleotide-gated channels and regulation of vertebrate phototransduction. J Exp Biol 204:2921–2931

Kumar P, Henikoff S, Ng PC (2009) Predicting the effects of coding non-synonymous variants on protein function using the SIFT algorithm. Nat Protoc 4:1073–1081. https://doi.org/10.1038/nprot.2009.86

Larkin MA et al (2007) Clustal W and Clustal X version 2.0. Bioinformatics 23:2947–2948. https://doi.org/10.1093/bioinformatics/btm404

Leconte L, Barnstable CJ (2000) Impairment of rod cGMP-gated channel alpha-subunit expression leads to photoreceptor and bipolar cell degeneration. Investig Ophthalmol Vis Sci 41:917–926

Li H, Durbin R (2010) Fast and accurate long-read alignment with Burrows-Wheeler transform. Bioinformatics 26:589–595. https://doi.org/10.1093/bioinformatics/btp698

Li M et al (2017) Structure of a eukaryotic cyclic-nucleotide-gated channel. Nature 542:60–65. https://doi.org/10.1038/nature20819

Maity S, Mazzolini M, Arcangeletti M, Valbuena A, Fabris P, Lazzarino M, Torre V (2015) Conformational rearrangements in the transmembrane domain of CNGA1 channels revealed by single-molecule force spectroscopy. Nat Commun 6:7093. https://doi.org/10.1038/ncomms8093

Marchesi A, Mazzolini M, Torre V (2012) A ring of threonines in the inner vestibule of the pore of CNGA1 channels constitutes a binding site for permeating ions. J Physiol 590:5075–5090. https://doi.org/10.1113/jphysiol.2012.238352

Marchesi A, Arcangeletti M, Mazzolini M, Torre V (2015) Proton transfer unlocks inactivation in cyclic nucleotide-gated A1 channels. J Physiol 593:857–870. https://doi.org/10.1113/jphysiol.2014.284216

Matulef K, Zagotta WN (2003) Cyclic nucleotide-gated ion channels. Ann Rev Cell Dev Biol 19:23–44. https://doi.org/10.1146/annurev.cellbio.19.110701.154854

Mazzolini M, Anselmi C, Torre V (2009) The analysis of desensitizing CNGA1 channels reveals molecular interactions essential for normal gating. J Gen Physiol 133:375–386. https://doi.org/10.1085/jgp.200810157

Mazzolini M et al (2018) The gating mechanism in cyclic nucleotide-gated ion channels. Sci Rep 8:45. https://doi.org/10.1038/s41598-017-18499-0

Meighan SE, Meighan PC, Rich ED, Brown RL, Varnum MD (2013) Cyclic nucleotide-gated channel subunit glycosylation regulates matrix metalloproteinase-dependent changes in channel gating. Biochemistry 52:8352–8362. https://doi.org/10.1021/bi400824x

Nair AV, Mazzolini M, Codega P, Giorgetti A, Torre V (2006) Locking CNGA1 channels in the open and closed state. Biophys J 90:3599–3607. https://doi.org/10.1529/biophysj.105.073346

Nair AV, Nguyen CH, Mazzolini M (2009) Conformational rearrangements in the S6 domain and C-linker during gating in CNGA1 channels. Eur Biophys J 38:993–1002. https://doi.org/10.1007/s00249-009-0491-4

Pepe IM (2001) Recent advances in our understanding of rhodopsin and phototransduction. Prog Retin Eye Res 20:733–759

Pifferi S, Boccaccio A, Menini A (2006) Cyclic nucleotide-gated ion channels in sensory transduction. FEBS Lett 580:2853–2859. https://doi.org/10.1016/j.febslet.2006.03.086

Schindelin J et al (2012) Fiji: an open-source platform for biological-image analysis. Nat Methods 9:676–682. https://doi.org/10.1038/nmeth.2019

Weitz D, Ficek N, Kremmer E, Bauer PJ, Kaupp UB (2002) Subunit stoichiometry of the CNG channel of rod photoreceptors. Neuron 36:881–889

Yang L et al (2015) Dependable and efficient clinical molecular diagnosis of chinese rp patient with targeted exon sequencing. PLoS ONE 10:e0140684. https://doi.org/10.1371/journal.pone.0140684

Zhong H, Molday LL, Molday RS, Yau KW (2002) The heteromeric cyclic nucleotide-gated channel adopts a 3A:1B stoichiometry. Nature 420:193–198. https://doi.org/10.1038/nature01201

Affiliations

Qing Gao[1] · Yifan Liu[1] · Xinlan Lei[1] · Qinqin Deng[1] · Yongqing Tong[2] · Lique Du[3] · Yin Shen[1]

[1] Eye Center, Renmin Hospital of Wuhan University, Wuhan 430060, Hubei, China

[2] Department of Clinical Laboratory, Renmin Hospital of Wuhan University, Wuhan 430060, Hubei, China

[3] BGI-Wuhan, Wuhan 430075, China